Supporting Information for

Valence Dependent Electrical Conductivity in a 3D Tetrahydroxyquinone Based Metal–Organic Framework

Gan Chen[1], Leland B. Gee[2], Wenqian Xu[3], Yanbing Zhu[4], Juan S. Lezama-Pacheco[5], Zhehao Huang[6], Zongqi Li[1], Jeffrey T. Babicz Jr.[2], Snehashis Choudhury[7], Ting-Hsiang Chang[7], Evan Reed[1], Edward I. Solomon[2,8], Zhenan Bao[7,*]

[1]Department of Materials Science and Engineering, Stanford University, Stanford, CA 94305, USA

[2]Department of Chemistry, Stanford University, Stanford, CA 94305, USA

[3]X-ray Science Division, Advanced Photon Source, Argonne National Laboratory, Lemont, IL 60439, USA

[4]Department of Applied Physics, Stanford University, Stanford, CA 94305, USA

[5]Department of Earth System Science, Stanford University, Stanford, CA 94305, USA

[6]Berzelii Centre EXSELENT on Porous Materials, Department of Materials and Environmental Chemistry, Stockholm University, SE-106 91 Stockholm, Sweden

[7]Department of Chemical Engineering, Stanford University, Stanford, CA 94305, USA

[8]Stanford Synchrotron Radiation Lightsource, SLAC National Accelerator Laboratory, Stanford University, Menlo Park, California 94025, USA

Contents

Methods S2

Additional Figures and Tables..... S4

References.....S13

Methods

Synthesis of FeTHQ

Tetrahydroxy-1,4-benzoquinone hydrate (THQ) and Iron (II) sulfate heptahydrate ($FeSO_4 \cdot 7H_2O$) were purchased from Sigma-Aldrich used without further purification. Tetrahydroxy-1,4-benzoquinone hydrate (THQ) (30 mg, 0.174 mmol on anhydrous basis) was dissolved in 5ml DMF + 5ml H_2O. The THQ solution was transferred into the solution of $FeSO_4 \cdot 7H_2O$ (96.9 mg, 0.348 mmol) in 10 mL H_2O in a 20ml vial. The vial was tightly sealed and then transferred into an 80 ^oC oven and kept in the oven for 12 hrs. Dark navy precipitate was obtained and filtered. The product was subsequently washed with H_2O (50 mL × 2) and acetone (20 mL × 2) and dried in 60 °C vacuum oven for 1 hour, yielding ~35 mg (83 %, assuming THQ is anhydrous) of FeTHQ powders. The product was stored in glovebox for further characterizations. Note with different batches of THQ ligand, slightly different conductivity and relative peak intensities in PXRD for FeTHQ are observed.

Reduction of FeTHQ

FeTHQ or FeTHQ_ox powders are vacuum dried at 60 °C oven for 1 hour prior to the reduction studies. Then 100 mg of FeTHQ powders are dispersed in anhydrous tetrahydrofuran (THF), to which the corresponding volume of freshly prepared 0.2 M sodium naphthalenide in THF was added slowly under stirring in the glovebox. The dispersion was kept stirred at room temperature for 12 hrs. Subsequently the dispersion is filtered, washed with nitrogen bubbled THF (50 mL × 2), methanol (50 mL × 2) and finally acetone (50 mL × 2). The reduced products were then dried 50 °C vacuum oven for 1 hour.

Activation of FeTHQ for BET

FeTHQ was prepared as previously described in **Synthesis of FeTHQ**, filtered and washed with water and acetone and dried at room temperature under vacuum. Then these FeTHQ powders were loaded to a BET tube and degassed at 60°C for 2 hours followed by 100°C for 8 hours prior to the nitrogen adsorption surface area measurement.

Conductivity measurement

The FeTHQ pellets (~200 μm thick with a diameter of ¼ inch) for the conductivity measurement were prepared by cold isostatic pressing using commercial pressing equipment (MTI). The measurement was performed under vacuum (ca. 10^{-4} Pa) to avoid the influence of oxygen and moisture. A linear four-contacts method (spacing between the contacts is 0.3 mm, the size of contact is 25 μm, contacts are made by Beryllium copper (BeCu)) was used to measure σ.[S1] Electrical conductivity measurement was carried out using a Keithley 4200 SCS parameter analyzer and the temperature control was realized by a CRX-6.5K Cryogenic Probe Station. σ was calculated from the current (I) and voltage (V) data according to the equation $\sigma = \frac{1}{C} \times (I/V) \times (\ln 2 / \pi \cdot t)$, where C is the geometry correction factor; [S1] t is the sample thickness.

Synchrotron powder XRD and crystal structure analysis

Synchrotron powder XRD measurement was performed at Beamline 17-BM of the Advanced Photon Source (APS) at the Argonne National Laboratory (ANL). FeTHQ powder was loaded in a Kapton® capillary tube of 1 mm diameter and measured with monochromatic X-ray (λ = 0.44811 Å) in the Debye-Scherrer

geometry using a VAREX XRD 4343CT flat panel detector. The 2D diffraction image collected by the detector was converted with the GSAS-II software[S2] to a 1D diffraction pattern, which was then used for structure determination and refinement through the TOPAS software.

Due to the difficulty in obtaining single crystals of FeTHQ, the PXRD data was used to analyze the crystal structure. Indexing of the FeTHQ diffraction pattern indicated a cubic unit cell with an axis length of 10.5457(2) Å and a probable space group of P23. The charge flipping method[S3] was applied in solving the structure and the result suggested the presence of 8 heavy atoms in one cell forming a cube shape, with each atom located at one vertex of the cube. The cube edge length was 3.8 Å, corresponding to twice of the Fe-O bond length, indicating a Fe-O-Fe apex-sharing geometry. Following this logic, an Fe octamer was constructed (Figure 1b) and the THQ ligand was located between two octamers (Figure 1c,d; Supplementary Video 1), which generated a diffraction pattern similar to the experimental one. The subsequent Rietveld refinement was performed (Figure 2a, Figure S1, Table S1) and the space group was changed to $Pm\bar{3}$ without any constraints in the final refinement.[S4]

Based on the synthesis, the solvent molecules ($Ow1$ and $Ow2$) are most likely DMF and/or water. The elemental composition indicated by the structure model is consistent with the experimental elemental analysis results (Table S2). Thermogravimetric analyses (TGA) of FeTHQ also confirmed a high content (> 8.6 %) of solvent molecules (Figure S3).

EXAFS data and fitting

Data was collected on beamline 11-2, at the Stanford Synchrotron Radiation Lightsource (SSRL). Measurements were performed in fluorescence mode at room temperature. Energy sweeps were done using a double crystal Si(220) monochromator, with one of the crystals detuned to 60% of the maximum intensity, to avoid harmonic contributions to the primary beam. Data analysis was performed using the Demeter software suit.[S5]

DFT calculations

Density functional theory (DFT) calculations were performed using the projected augmented wave (PAW) method[S6] as implemented in the Vienna Ab Initio Simulation Package (VASP).[S7] The generalized gradient approximation (GGA) functional of Perdew, Burke, and Ernzerhof (PBE) were used for the electron exchange and correlation effects.[S8] A plane-wave basis set with a kinetic energy cut-off of 520 eV was used. The Brillouin zone was sampled using a 4x4x4 **Γ**-centered Monkhorst-Pack k-points grid[S9] and tested for convergence.

Diffuse reflectance spectroscopy

Diffuse reflectance spectra between 200 and 1800 nm were collected on a CARY 6000i UV-Vis-NIR spectrophotometer at a scan rate of 600 nm/min. 0.25 wt% of FeTHQ powders were ground with KBr in a mortar and pressed into pellets for measurement. A baseline was collected on pure KBr pellet prior to each sample measurement.

Mössbauer spectroscopy

^{57}Fe Mössbauer spectroscopy was performed using a SEE Co. W202 gamma-ray spectrometer operating with a Janis SVT400 high efficiency LHe/LN2 cryostat utilizing ^{57}Co in a rhodium matrix as the gamma-ray source. All spectra were collected at zero applied magnetic field. The sample was held nominally at 80 K

or 6 K with liquid helium. Isomer shifts quoted relative to α-Fe foil at 298 K. Fits of quadrupole doublets to the obtained spectrum were conducted with the MossWinn software.[S10]

Other characterizations

Powder X-ray diffraction was carried out on a Rigaku MiniFlex 600 benchtop X-ray powder diffractometer equipped with a Cu sealed tube (λ = 1.54178 Å) at 40 kV and 15 mA. Scanning electron microscopy (SEM) analysis was done on a field emission-scanning electron microscope (Magellan 400 XHR) at 5 kV. Transmission electron microscopic (TEM) observation was performed on a JEOL JEM2100 microscope, and operated at 200 kV (Cs 1.0 mm, point resolution 0.23 nm). Images were recorded with a Gatan Orius 833 CCD camera (resolution 2048 x 2048 pixels, pixel size 7.4 µm) under low dose conditions. Thermogravimetry analyses (TGA) were run with a nitrogen flow rate of 10 ml min^{-1} on a TA Instrument Q500 Thermogravimetric Analyzer, using a heating rate of 10 °C min^{-1}. Elemental analyses (C, H, and N) were obtained from Atlantic Microlab, Inc. Inductively coupled plasma-optical emission spectrometry (ICP-OES) was carried out on a Thermo Scientific ICAP 6300 Duo View Spectrometer. Gas adsorption measurements were measured using Autosorb IQ3. Riken AC-2 photoelectron spectrometer was used for PESA measurements. X-ray photoelectron spectroscopy (XPS) was done on a PHI Versaprobe III with an Al K-alpha radiation.

Additional figures and tables

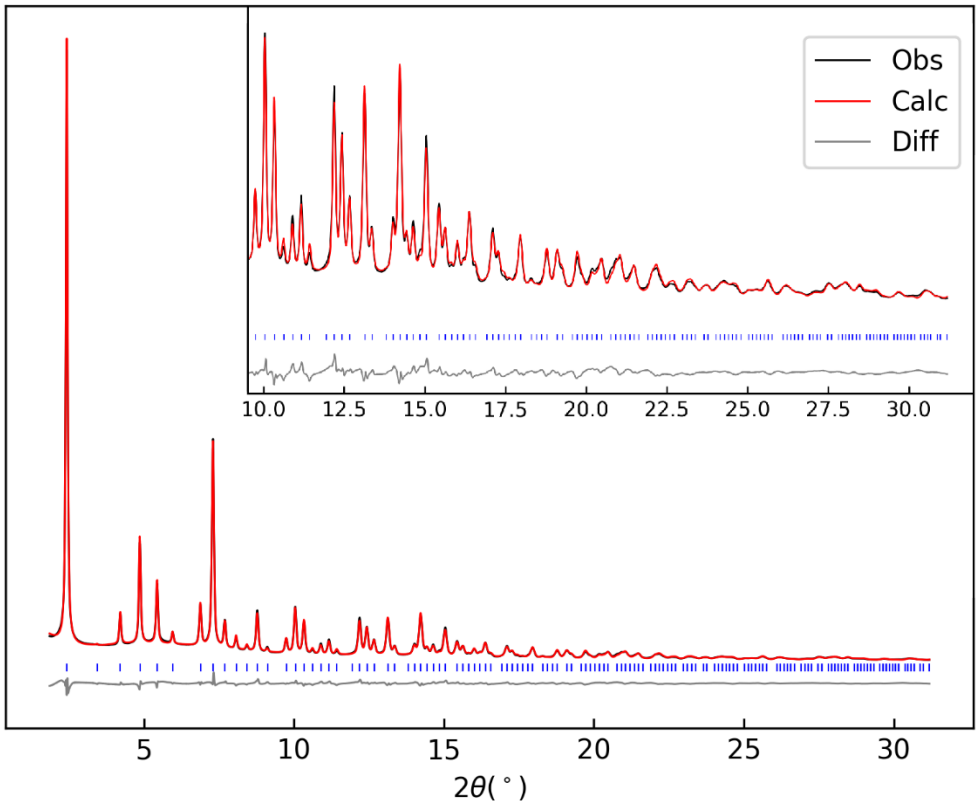

Figure S1. Full PXRD Refinement plot of FeTHQ

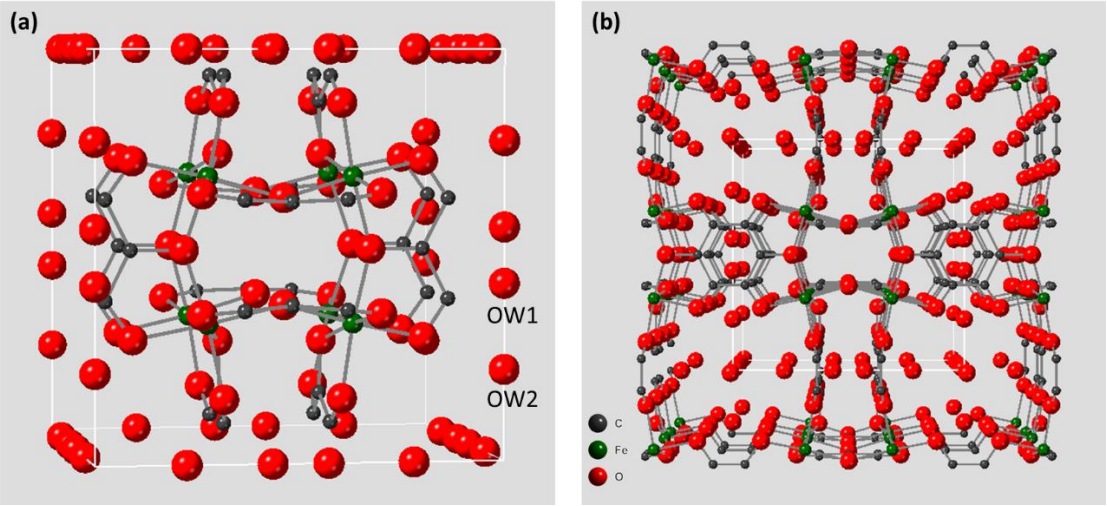

Figure S2. (a) Unit cell and (b) expanded network structure for FeTHQ including solvent/water molecules

Table S1. Crystallographic data and refinement statistics

Chemical Name	FeTHQ
Crystal system	Cubic
Space Group	$P\,m\,\bar{3}$
a (Å)	10.5457(2)
V (Å^3)	1172.80(7)
Temperature (K)	298
Wavelength (Å)	0.44811
Refinement d_{min} (Å)	0.834
R_{wp}	0.0319
R_p	0.0256
Goodness of fit (χ^2)	4.485

Table S2. Experimental and theoretical elemental composition of FeTHQ. C, H and N content are obtained by elemental analysis and Fe content is measured by ICP-OES, O content is calculated assuming no other elements are present in the sample. The formula of the MOF is assumed to be $Fe_8(C_6O_6)_6(H_2O)_{10}(DMF)_{1.6}$, which agrees well with the elemental analysis results from two batches of FeTHQ (FeTHQ1 and FeTHQ2).

Sample	C (wt%)	H (wt%)	N (wt%)	Fe (wt%)	O (wt%)
FeTHQ1	25.06	1.67	1.22	24.91	47.14
FeTHQ2	24.53	1.75	1.30	25.99	46.43
$Fe_8(C_6O_6)_6(H_2O)_{10}(DMF)_{1.6}$	27.97	1.79	1.28	25.50	43.46

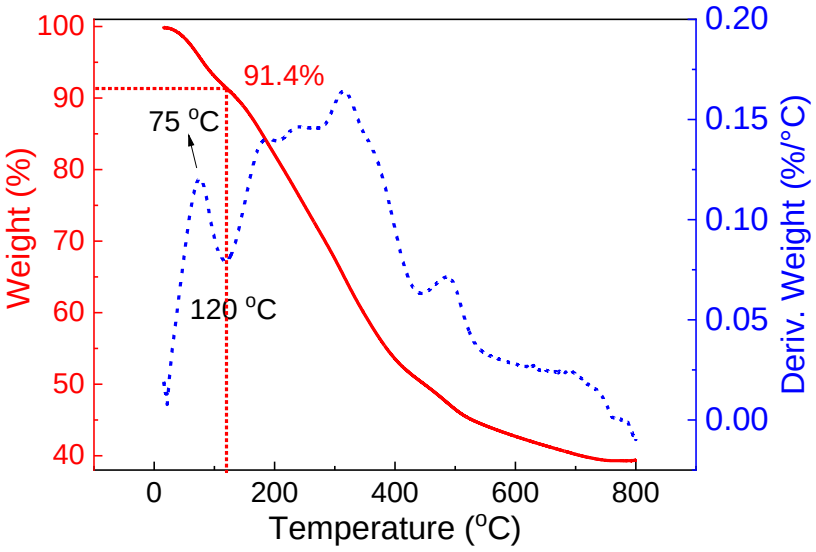

Figure S3. TGA curve for FeTHQ.

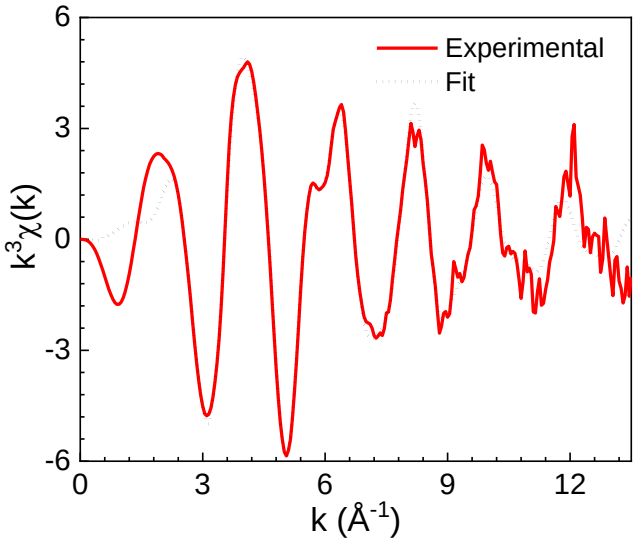

Figure S4. k-Space EXAFS spectra of FeTHQ

Table S3. EXAFS fitting results. The coordination numbers (N*) are from the CIF file.

	Fe-O1	Fe-C1	Fe-O2	Fe-Fe1	Fe-O3	Fe-C2	Fe-O4
N*	6	6	3	3	3	6	6
D(Å)	2.03(1)	2.79(2)	3.66(6)	3.89(2)	3.83(15)	4.07(10)	4.87(10)
σ^2(Å)	0.0078(1)	0.0105(20)	0.0133(90)	0.0102(30)	0.0133(92)	0.0153(92)	0.0153(92)
S_0^2	0.82 ± 0.06						
ΔE_0 (eV)	1.1 ± 0.9						
R-factor	0.006						

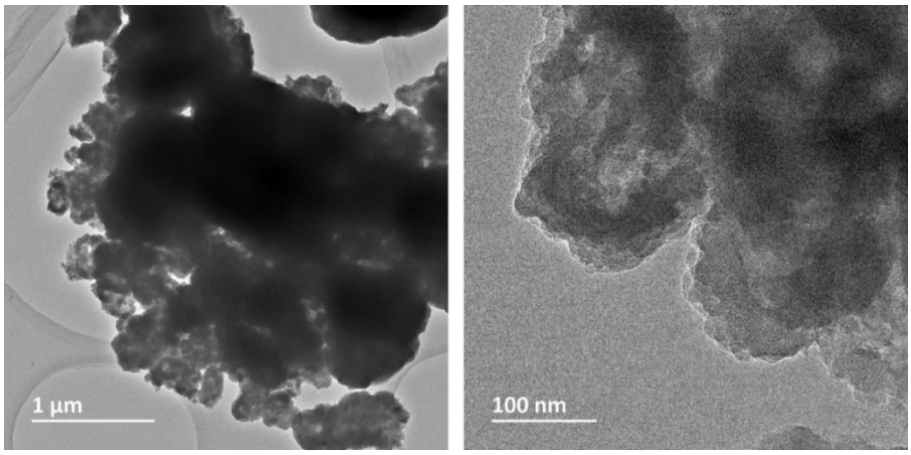

Figure S5. TEM images of FeTHQ, which show that the crystals have spherical morphology and severe intergrowth. In the left image, several spherical particles with diameters around 1 µm and many smaller particles with the size of hundreds of nanometers are interconnected to form the 3 µm large particle. And even within the small particles (shown on the right), there are many grain boundaries.

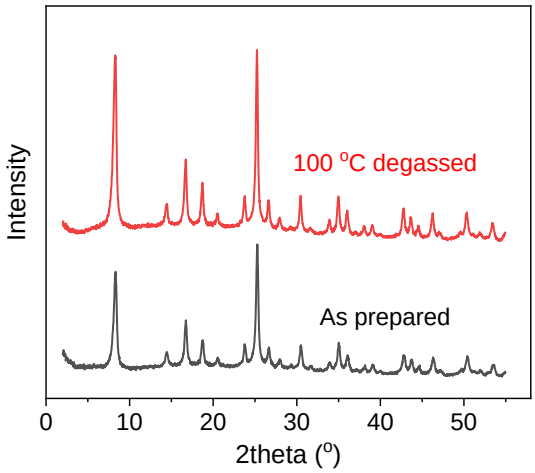

Figure S6. PXRD data for the as prepared FeTHQ and FeTHQ degassed at 100 for 8 hrs

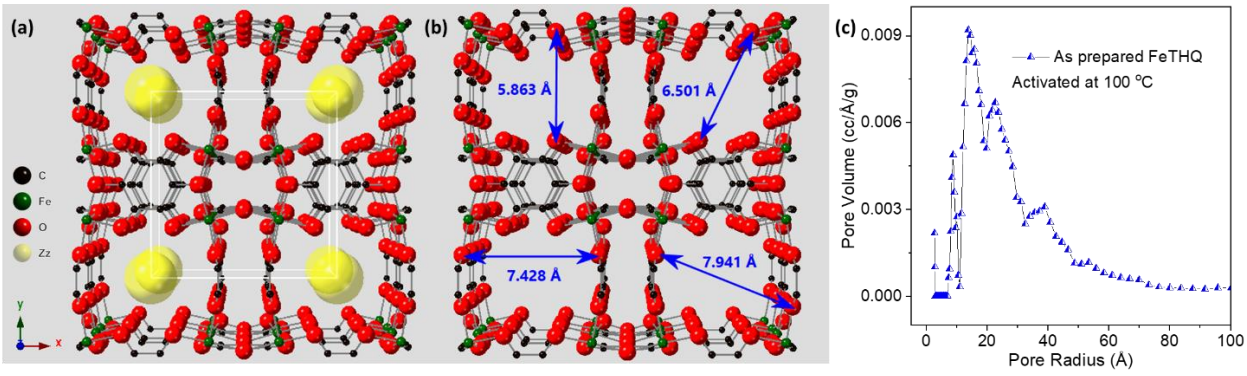

Figure S7. (a) cavities (yellow spheres) in fully activated FeTHQ MOF, of which the radius is calculated to be 3.726 Å; (b) O-O distances surrounding the oval channels in FeTHQ; (c) pore size distribution calculated by DFT method for FeTHQ activated at 100 °C.

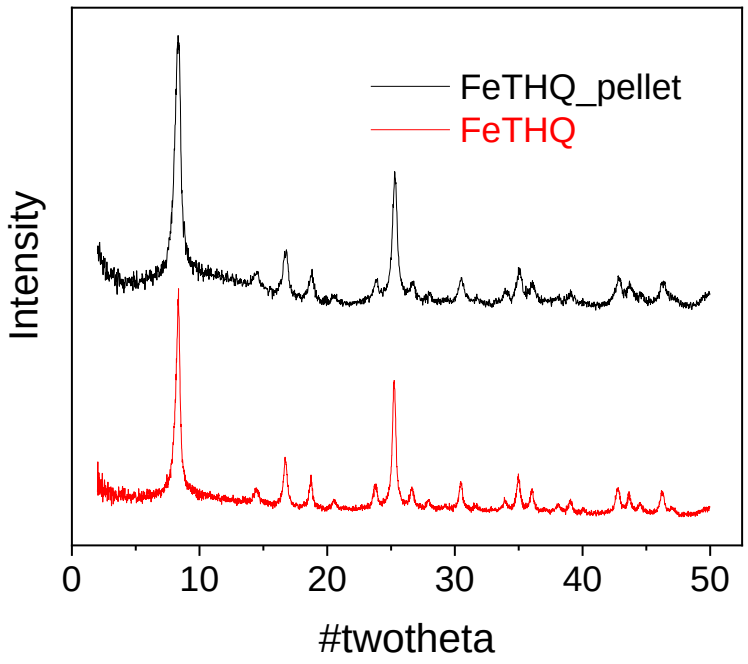

Figure S8. PXRD for FeTHQ and FeTHQ pellet samples

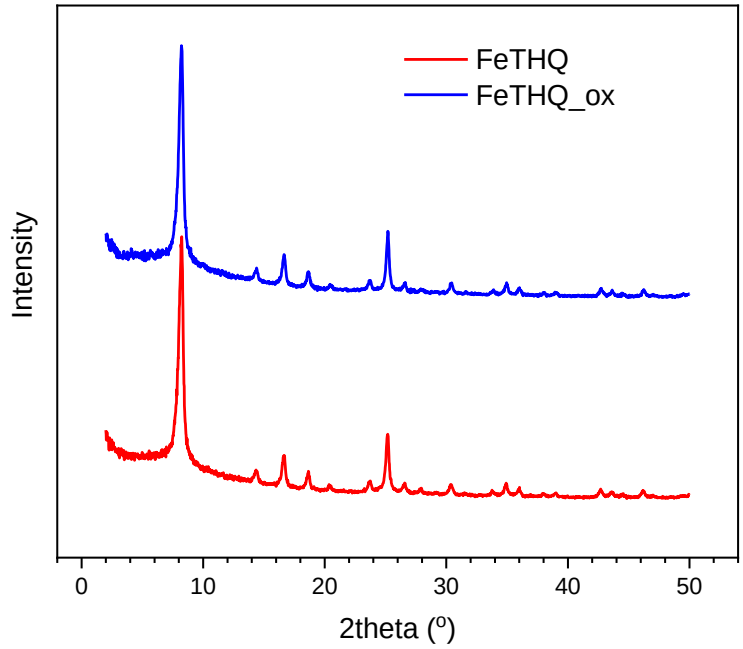

Figure S9. PXRD of the as prepared FeTHQ and air oxidized FeTHQ_ox sample.

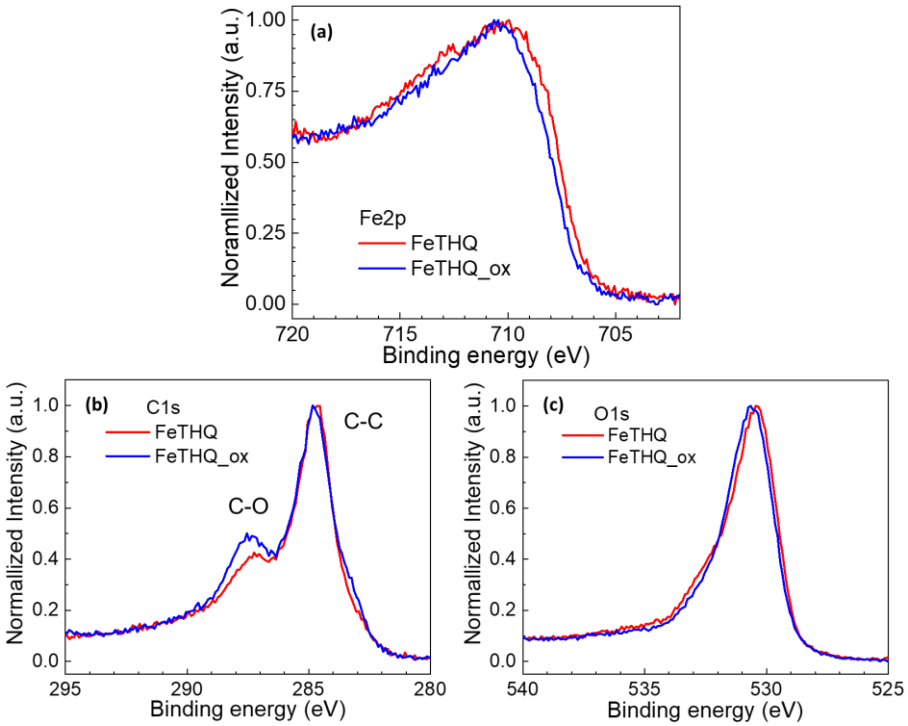

Figure S10. (a) Fe2p, (b) C1s and (c) O1s high resolution XPS of FeTHQ and FeTHQ_ox. In FeTHQ_ox, the O1s spectrum exhibits a very slight shift (~ 0.2 eV) towards higher binding energy and the C1s gives a higher portion of C-O.

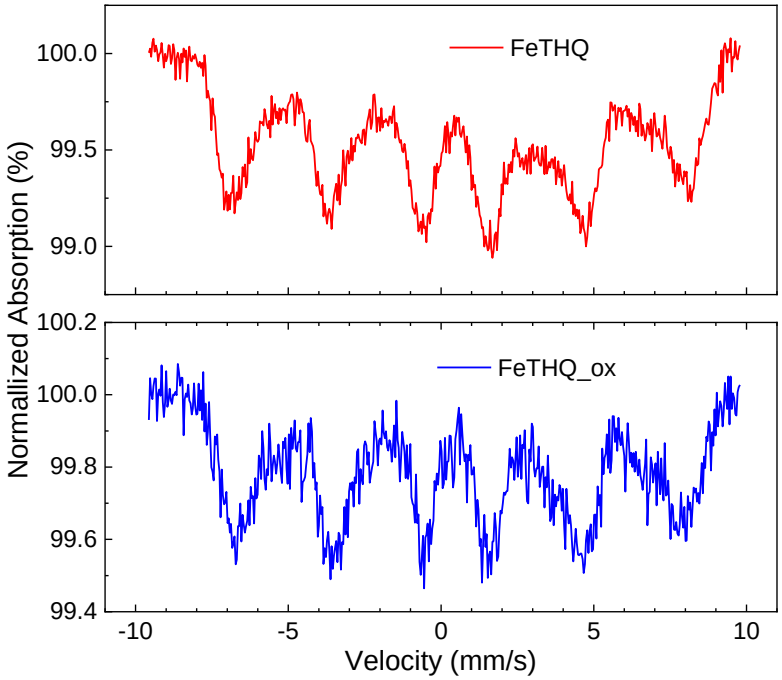

Figure S11. Zero applied field Mössbauer Spectra of FeTHQ and FeTHQ_ox at 6 K. Besides signal-to-noise there are not significant differences in the spectra. The spectra are both indicative of a dominantly high-spin ferric species that is split by magnetic hyperfine interactions.

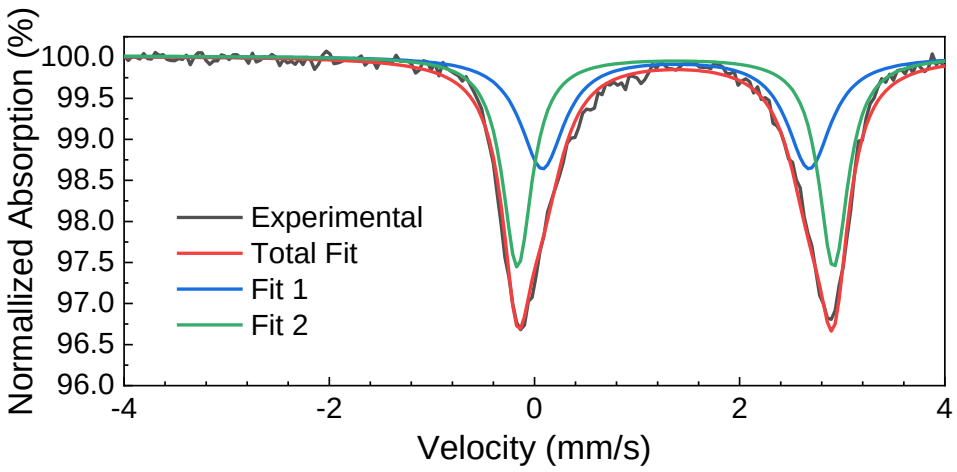

Figure S12. Mössbauer Spectroscopy of FeTHQ filtrate control sample at 80 K. This control sample was prepared by evaporating the solvents with the help of a cold trap and reduced pressure (oil pump), such that minimum exposure of the sample to air was achieved. The spectrum differs significantly from that of the FeTHQ MOF. And there is no indication for any ferric species in the filtrate. The very different parameters for the ferrous species in the filtrate control (Table S4) from that in the FeTHQ MOF indicate that the species observed in the MOF are not unreacted ferrous sulfate precursor species in the solvent.

Table S4. Mössbauer parameters derived from fitting each spectrum. All units in mm/s. Standard deviation in parentheses.

Sample	Species	Percent	Isomer Shift	Quadruple Splitting	Linewidth
FeTHQ	Ferric	68.2	0.54 (0.0016)	0.95 (0.0030)	0.41 (0.0026)
	Ferrous 1	28.5	1.10 (0.0049)	2.45 (0.0076)	0.57 (0.0137)
	Ferrous 2	3.3	1.48 (0.0107)	2.77 (0.0205)	0.22 (0.0241)
FeTHQ_ox	Ferric	85.9	0.54 (0.0024)	0.95 (0.0048)	0.46 (0.0039)
	Ferrous 1	7.8	0.95 (0.0170)	2.47 (0.0176)	0.37 (0.0416)
	Ferrous 2	6.3	1.25 (0.0079)	2.28 (0.0212)	0.25 (0.0240)
FeTHQ_red4	Ferric	42.8	0.52 (0.0025)	0.91 (0.0047)	0.45 (0.0065)
	Ferrous	57.2	1.19 (0.0019)	2.57 (0.0037)	0.46 (0.0057)
FeTHQ_redox0.5	Ferric	75.7	0.54 (0.0014)	0.95 (0.0027)	0.43 (0.0038)
	Ferrous	24.3	1.07 (0.0071)	2.41 (0.0142)	0.60 (0.0233)
FeTHQ_redox2	Ferric	54.5	0.53 (0.0022)	0.94 (0.0044)	0.43 (0.0048)
	Ferrous	45.5	1.18 (0.0034)	2.47 (0.0068)	0.52 (0.0090)
FeTHQ filtrate	Ferrous 1	44.2	1.378 (0.003)	2.600 (0.026)	0.518 (0.015)
	Ferrous 2	55.8	1.374 (0.001)	3.082 (0.007)	0.347 (0.010)

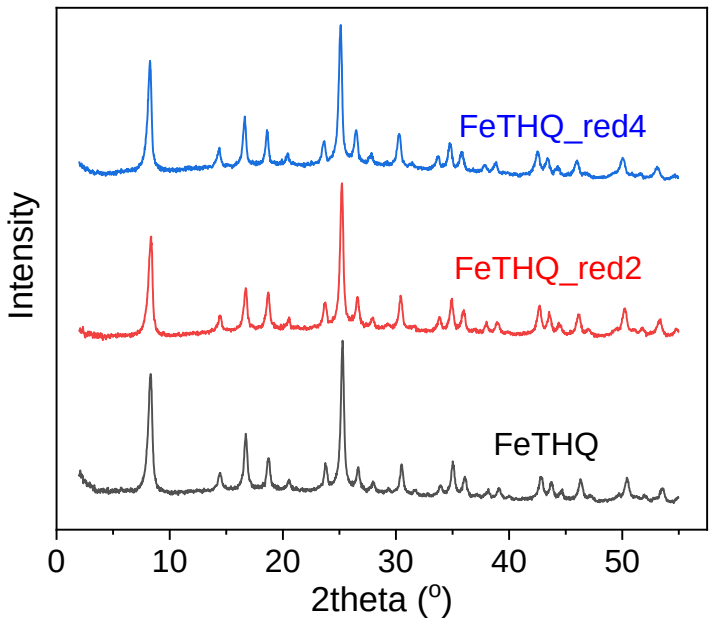

Figure S13. PXRD for as prepared and reduced FeTHQ samples

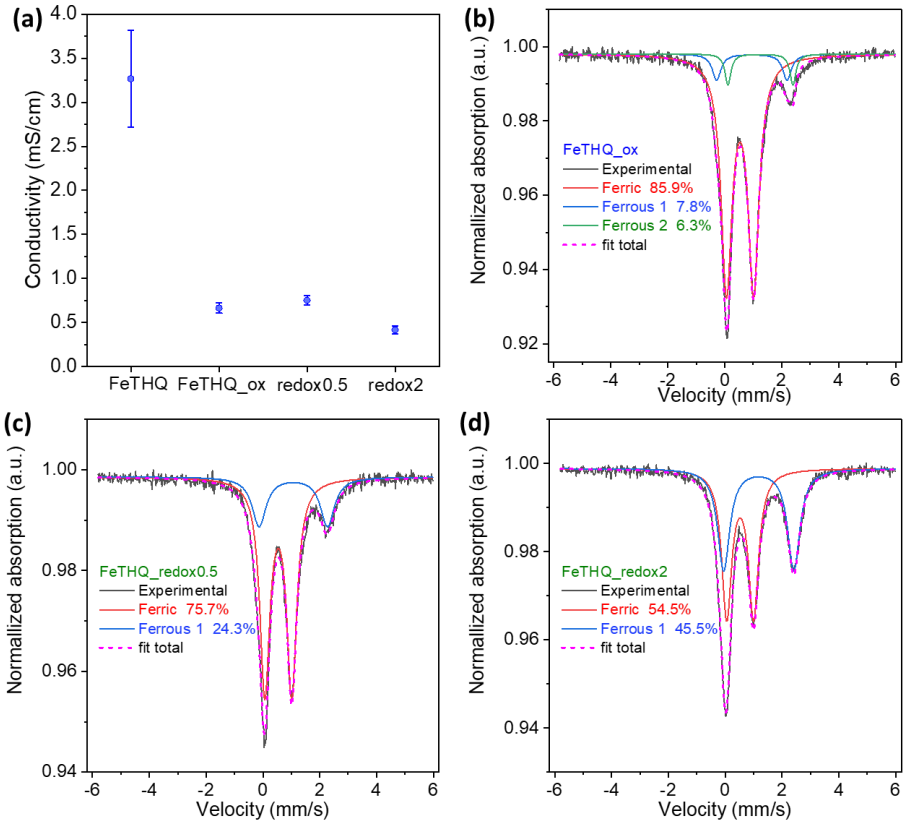

Figure S14. Reduction of FeTHQ_ox with sodium naphthalenide. (a) Conductivity values for: FeTHQ—as prepared, FeTHQ_ox—air oxidized for two weeks, FeTHQ_redox0.5/2—100 mg air oxidized FeTHQ reduced with 0.5/2 ml 0.2 M freshly prepared NaC_8H_{10}; Mössbauer spectroscopy for (b) FeTHQ_ox, (c) FeTHQ_redox0.5 and (d) FeTHQ_redox2 at 80 K. Mössbauer spectroscopy showed that Fe^{3+} in FeTHQ_ox can be reversibly reduced back to Fe^{2+}; however, the conductivity showed very limited recover from the

decrease caused by oxidation. The irreversibility for conductivity change is not related to material degradation as no noticeable structural change was observed in PXRD after the whole oxidation-reduction process (Figure S15), but rather again due to the heterogenous nature of the reduction reaction versus the more homogenous air oxidation process.

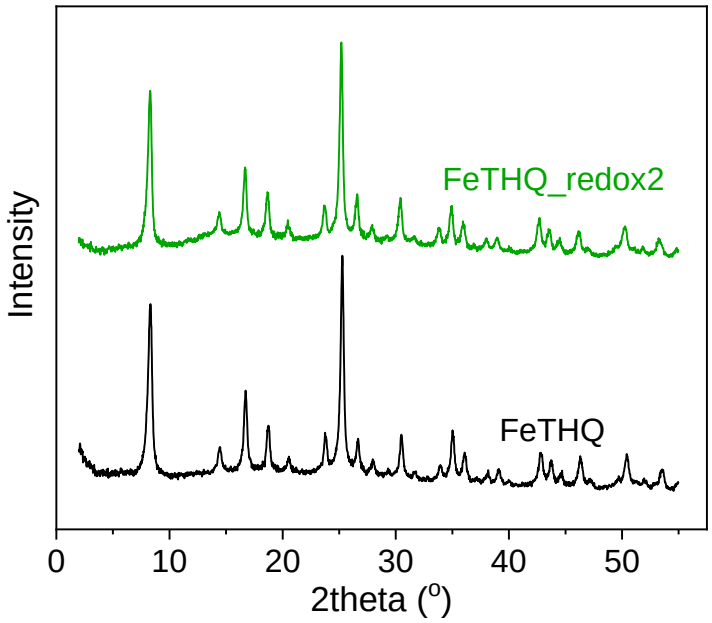

Figure S15. PXRD for as-prepared FeTHQ and FeTHQ_redox2 samples. No noticeable structural change was observed in PXRD after the whole oxidation-reduction process

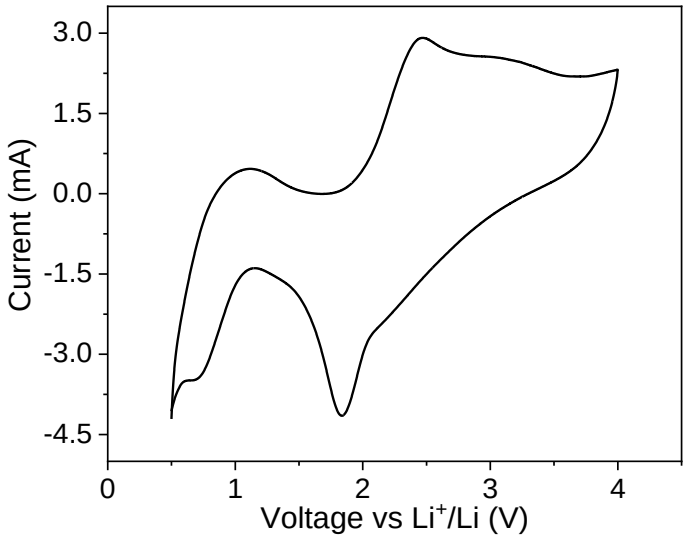

Figure S16. Cyclic voltammogram of FeTHQ in a coin cell with Li metal as the anode and FeTHQ as the cathode. Scan rate 10 mV/s. Cathode were prepared by mixing FeTHQ powders with carbon black conductive additive (Super C65, TIMCAL) and polytetrafluoroethylene (PVDF) binder in the mass ratio of 80:10:10.

References

(1) Smits, F. M., *The Bell System Technical Journal* **1958,** *37* (3), 711-718.
(2) Toby, B. H.; Von Dreele, R. B., *J. Appl. Crystallogr.* **2013,** *46* (2), 544-549.
(3) Coelho, A., *Acta Crystallographica Section A* **2007,** *63* (5), 400-406.
(4) Spek, A., *J. Appl. Crystallogr.* **2003,** *36* (1), 7-13.
(5) Ravel, B.; Newville, M., *Journal of Synchrotron Radiation* **2005,** *12* (4), 537-541.
(6) Kresse, G.; Joubert, D., *Phys. Rev. B* **1999,** *59* (3), 1758-1775.
(7) (a) Kresse, G.; Furthmüller, J., *Phys. Rev. B* **1996,** *54* (16), 11169-11186. (b) Blöchl, P. E., *Phys. Rev. B* **1994,** *50* (24), 17953-17979.
(8) Perdew, J. P.; Burke, K.; Ernzerhof, M., *Phys. Rev. Lett.* **1996,** *77* (18), 3865-3868.
(9) Monkhorst, H. J.; Pack, J. D., *Phys. Rev. B* **1976,** *13* (12), 5188-5192.
(10) Klencsár, Z., *Hyperfine Interact.* **2013,** *217* (1-3), 117-126.